

NRC-CNRC CONSTRUCTION

Evaluation of Low-Cost CO₂ Sensors

Author(s): Carsen Banister, Justin Berquist, Talal
Toushan

Report No.: A1-009645.4

Report Date: 14 March 2019



© (2019) Her Majesty the Queen in Right of Canada,
as represented by the National Research Council Canada.

Cat. No. NR24-35/2019-E
ISBN 978-0-660-30028-3



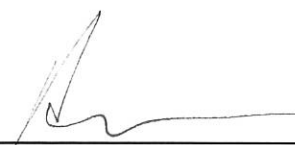
Evaluation of Low-Cost CO₂ Sensors

Author



Carsen Banister, Ph.D.

Approved



Anne Barker, MSc
Program Leader
Arctic Program
NRC Ocean, Coastal and River Engineering

Report No.: A1-009645.4
Report Date: 12 February 2019
Contract No.: A1-009645
Agreement Date: 1 April 2016
Program: Arctic

35 pages

Copy no. 1 of 2

This report may not be reproduced in whole or in part without the written consent of the National Research Council Canada and the Client.

Table of Contents

List of Figures	ii
List of Tables.....	iii
Executive Summary	iv
1 Introduction.....	1
2 Literature Review.....	2
3 Materials and Methods	3
3.1 Apparatus	3
3.2 Sensors Tested	3
3.3 Data Collection	5
3.4 Experimental Methodology	5
4 Results.....	7
4.1 Verifying Chamber Performance	7
4.2 Reference CO ₂ Sensor Calibration.....	7
4.3 CO ₂ Sensor Testing Sample Results.....	8
4.5 Steady-State Accuracy	11
4.5.1 Detailed Accuracy Analysis	13
4.6 Hysteresis.....	17
4.7 Repeatability.....	18
4.7.1 Standard Deviation Analysis	21
5 Discussion	23
6 Conclusion.....	24
7 Future Work.....	25
Acknowledgments.....	26
Appendix A - Reference Sensor Calibration Data.....	28
Appendix B - Data Tables	29
B.1 Accuracy.....	29
B.2 Hysteresis.....	32
B.3 Repeatability.....	33

List of Figures

Figure 1. Two reference CO ₂ sensors installed in the test chamber	3
Figure 2. Sensor type A	4
Figure 3. Sensor type B	4
Figure 4. Sensors connected to Arduino microcontrollers	5
Figure 5. Sensors and data acquisition hardware placed in the test chamber	6
Figure 6. 300 ppm CO ₂ cylinder connected to mass flow controller and chamber	6
Figure 7. Increasing calibrated gas flow rate test	7
Figure 8. Vaisala GMD20 sensor readings	8
Figure 9. Sensors type A readings, day 1	10
Figure 10. Sensor type B readings, day 1	10
Figure 11. Sensor type A readings, all three days	12
Figure 12. Sensor type B readings, all three days	12
Figure 13. Sensors types A & B readings, all three days	13
Figure 14. Sensor type A percentage error	14
Figure 15. Sensor type B percentage error	15
Figure 16. Sensor type A deviation error	15
Figure 17. Sensor type B deviation error	16
Figure 18. Sensor type A percentage error analysis	17
Figure 20. Sensor type A deviation error analysis	17
Figure 19. Sensor type B percentage error analysis	17
Figure 21. Sensor type B deviation error analysis	17
Figure 22. Sensor type A hysteresis analysis	18
Figure 23. Sensor type B hysteresis analysis	18
Figure 24. Sensor type A repeatability	20
Figure 25. Sensor type B repeatability	20
Figure 26. Sensor type A repeatability analysis (increasing)	21
Figure 27. Sensor type A repeatability analysis (decreasing)	21
Figure 28. Sensor type B repeatability analysis (increasing)	21
Figure 29. Sensor type B repeatability analysis (decreasing)	21
Figure 30. Sensor type A standard deviation	22
Figure 31. Sensor type B standard deviation	22
Figure 32. Sensor type A hysteresis	32
Figure 33. Sensor type B hysteresis	32

List of Tables

Table 1. Vaisala GMD20 sensor readings	28
Table 2. Sensor specifications	28
Table 3. Sensor type A standard deviation	29
Table 4. Sensor type B standard deviation	29
Table 5. Sensor type A percentage error	29
Table 6. Sensor type A deviation error	30
Table 7. Sensor type B percentage error	31
Table 8. Sensor type B deviation error	31
Table 9. Sensor type A hysteresis	33
Table 10. Sensor type A repeatability (increasing)	33
Table 11. Sensor type A repeatability (decreasing)	33
Table 12. Sensor type B repeatability (increasing)	33
Table 13. Sensor type B repeatability (decreasing)	33

Executive Summary

Demand-controlled ventilation (DCV) systems use indicators of demand for ventilation, such as excess carbon dioxide, to control a ventilation system. DCV denotes continuously and automatically adjusting the ventilation rate in response to indoor pollutant concentrations. DCV systems have the potential to ventilate more at times when it provides an indoor air quality (IAQ) advantage and less when it provides an energy advantage (during vacancy). The focus of the work presented here is to evaluate the performance of two selected low-cost CO₂ sensors to verify their suitability in the control of residential ventilation systems.

DCV systems are typically only used in commercial applications. The cost of conventional DCV systems is prohibitive for smaller applications, such as residential, driving the need for low-cost components. As most new and retrofit building construction becomes more airtight, the need for effective and efficient ventilation of residential spaces becomes even more important.

Laboratory testing of sensors was completed using a sealed chamber and calibrated gas sources with controlled CO₂ concentrations. Three sensors were considered, but only two were tested in detail due to the clear inaccuracy and unsuitability of one of the sensors. The sensor that was ruled out early used micro-hotplate technology for gas sensing, but was not found to provide any useful results.

It was found that the two sensors tested in detail have suitable accuracy, repeatability, and hysteresis to be used in ventilation control systems. The sensors are both non-dispersive infrared type and had typical error of +/- 10% at the key area of interest for indoor air quality of 500-1500 ppm. This work shows that ultra-low cost CO₂ sensors in the area of \$25 CAD each may not be suitable for ventilation system control, but that low cost CO₂ sensors in the range of \$50-100 CAD would be suitable for developing a low cost controller and sensor package for managing indoor CO₂ concentration below a maximum acceptable limit.

1 Introduction

Building performance and airtightness continue to increase, and thus the need for efficient and reliable air ventilation systems is becoming ever more important. A ventilation system distributes fresh outdoor air throughout a building and discharges stale indoor air to maintain the quality of the indoor environment suitable for the safety and health of occupants [1]. A building's ventilation requirements can vary greatly depending on the occupancy and use over the course of a day, week or season. As a result, many control strategies for operating ventilation systems have been developed and studied in detail. Despite this, it remains very uncommon to have demand-controlled ventilation strategies in residential buildings due to the unavailability and/or high cost of the sensors and controllers required to do so.

Carbon dioxide (CO₂) is commonly used as the sensing agent within demand-controlled ventilation systems. CO₂ sensors measure the indoor air CO₂ concentration at some location within the building or ventilation system. These measurements are then used to control the air flow rate in the system through the utilization of a modulating damper or by varying the fan speed. The accuracy of such CO₂ concentration measurements is important since inaccuracy may result in improper ventilation. For example, incorrect high CO₂ readings will result in excessive ventilation, requiring extra energy to condition the air. On the other hand, incorrect low sensor readings will result in under-ventilation, resulting in poor indoor air quality [2].

2 Literature Review

Fahlen, Andersson, and Ruud (1992) studied two non-dispersive infra-red (NDIR) CO₂ sensors [3]. One of the CO₂ sensors was a photo-acoustic type and the other was an infrared spectroscopy type. The error-margin between each sensor's reading and the actual concentration was within ± 50 ppm at 1000 ppm CO₂. However, the sensor measurements deviated from the actual concentration by up to ± 200 ppm at a concentration level of 2000 ppm, or $\pm 10\%$.

Fisk, Faulkner, and Sullivan (2007) assessed the accuracy of forty-four CO₂ sensors placed in nine commercial buildings to evaluate their performance and reliability [4]. They found wide variations in the sensors' measurements and sometimes the error was as much as several hundred parts per million. The authors concluded that the accuracy of these CO₂ sensors was inadequate, and better sensor maintenance and calibration were needed.

Pandey, Kim, and Lee (2007) conducted experiments to examine the performance of two types of NDIR CO₂ sensors (six sensors of each type) [5]. They performed their tests in an enclosed chamber at concentrations simulating typical CO₂ levels in building environments (500 ppm and 1000 ppm) at various flow rates. The results showed excellent accuracy (within 5%), and the correlation coefficients for all sensors were approximately 1 ($r > 0.999$, $p = 0.01$). They concluded that the sensors tested were reliable and suitable for measuring CO₂ levels in the atmosphere and building environments.

Shrestha and Maxwell (2010) evaluated the performance of forty-five sensors; three sensor types, fifteen of each model [6]. Among the fifteen models tested, eight models had a single-lamp, single-wavelength configuration; four models had a dual-lamp, single-wavelength configuration, and three models had a single-lamp, dual-wavelength configuration. The authors found a remarkable deviation in the sensors' behavior – no sensor models met their manufacturer specifications in terms of accuracy for all types of sensors.

Shrestha and Maxwell (2010) conducted further and more comprehensive analyses to evaluate the performance of the aforementioned sensors at various relative humidity, temperature, and pressure levels used in building heating, ventilation and air conditioning (HVAC) applications [7]. They concluded that there is a big difference in humidity, temperature, and pressure sensitivity of different models of CO₂ sensors. Moreover, they found wide variations in sensor performance among sensors within the same model type.

The reviewed literature displays that there is an interest in investigating the performance of CO₂ sensors to be used in ventilation system control. There are mixed results from the summarized studies: some studies conclude that the sensors have suitable accuracy and others demonstrate that many sensors do not meet manufacturer specifications. Given the various conclusions and the rapidly evolving field of microcontrollers and sensors, there was interest in studying the performance of readily available CO₂ sensors of cost in the range of \$80-100 USD to assess suitability in building ventilation control. This study investigates two CO₂ sensors for their application in airtight buildings in cold, harsh climates, since high thermal loads are associated with conditioning the ventilation air.

3 Materials and Methods

This section describes the apparatus utilized to test the suitability of the two selected low-cost CO₂ sensors for residential demand-controlled ventilation, explains the experimental methodology used, and describes how data was collected.

3.1 Apparatus

A lab-grade sensor calibration chamber was utilized for the testing of the two CO₂ sensors, shown in Figure 1. The chamber is made of aluminum and was fabricated in-house at the National Research Council Canada (NRC). The calibration chamber has holes on the top to enable the installation of external, calibrated sensors for further verification and measurement. On the back of the chamber there are two ports that allow for calibrated gas to enter and exit the chamber. The gas passes through a perforated tube as it is injected, spreading the gas throughout the chamber. Displaced gas exits the chamber via a similar perforated tube and is discharged through a ventilation hood within the laboratory. On the front of the chamber is a panel that can be removed in order to place the sensors inside. The front panel can be fastened to the chamber via sixteen screws and includes an o-ring to ensure a proper seal.

To further verify the chamber CO₂ concentration, two reference CO₂ sensors (Vaisala GMD20) with an accuracy of $\pm (40 \text{ ppm} + 2\% \text{ of reading})$ [8] were installed and their outputs measured against three CO₂ concentrations; 300 ppm, 1050 ppm and 2500 ppm. Figure 1 shows the Vaisala GMD20 sensors installed on the top of the test chamber. Their voltage outputs were measured using a multi-meter to have reference CO₂ readings.

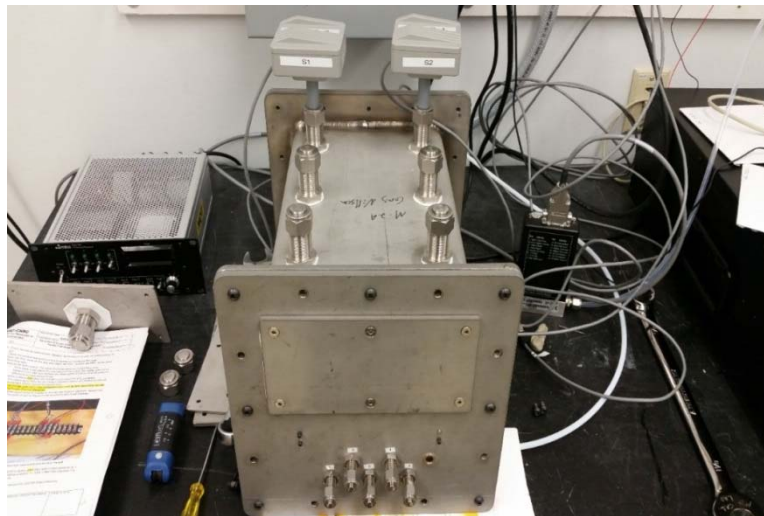


Figure 1. Two reference CO₂ sensors installed in the test chamber

3.2 Sensors Tested

Three models of CO₂ sensors were considered for this study. Only two of the models were tested in detail because the third did not produce any useable results. Various concentrations of CO₂ were injected into a well-sealed chamber to produce calibration relationships and assess their linearity, accuracy, hysteresis, and repeatability.

The first model, sensor type A (Gravity SEN0219), shown in Figure 2, is an infrared high-precision analog output sensor based on NDIR technology. An accuracy of $\pm (50 \text{ ppm} + 3\% \text{ of the reading})$ is stated in the

specifications for this sensor [9]. It has good selectivity and oxygen-free dependency. It has temperature compensation and an analog voltage output. It is compatible with microcontrollers or other devices that have an analog-to-digital converter (ADC) capability [9].

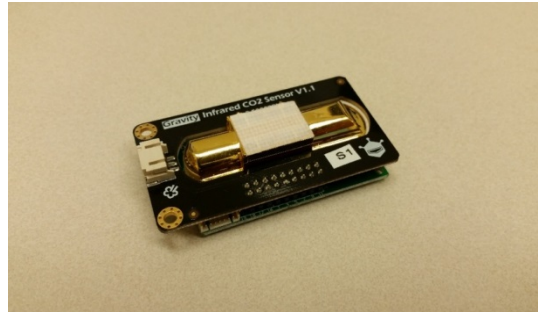


Figure 2. Sensor type A

The second model tested, sensor type B (Grove MH-Z16), shown in Figure 3, is an infrared CO₂ sensor which also uses NDIR technology with built-in temperature sensor and has a UART output. An accuracy of $\pm (50 \text{ ppm} + 5\% \text{ of the reading})$ is stated in the specifications for this sensor [10]. It also has good selectivity, and is commonly used in HVAC and indoor air quality monitoring [11]. For in-duct measurements of CO₂ concentration, it may have a favourable form factor since it can be easily mounted in the airflow.



Figure 3. Sensor type B

The third model which was considered initially, but not tested in detail, is shown below in Figure 4.



Figure 4. Sensor type C

3.3 Data Collection

Arduino microcontrollers were used to read the outputs from the sensors. The type A sensors were connected to an Arduino MKR1000 microcontroller and the type B sensors were connected to Arduino Mega and Due microcontrollers. Real-time clocks and SD cards were also used for the purpose of data logging.

The ADC used for reading type A sensors has a 10-bit resolution, meaning that there are 1024 potential values within the voltage range selected. A reference voltage of 2.23 V was used for the analog voltage readings, giving a resolution of 2.180 mV. This voltage resolution corresponds to a CO₂ concentration of 6.8 ppm, which is significantly less than the uncertainty expected from variations in sensor accuracy.

Figure 5 shows the chamber ready sensor configuration; the two sensor types connected to the Arduino microcontrollers and data logging electronics.

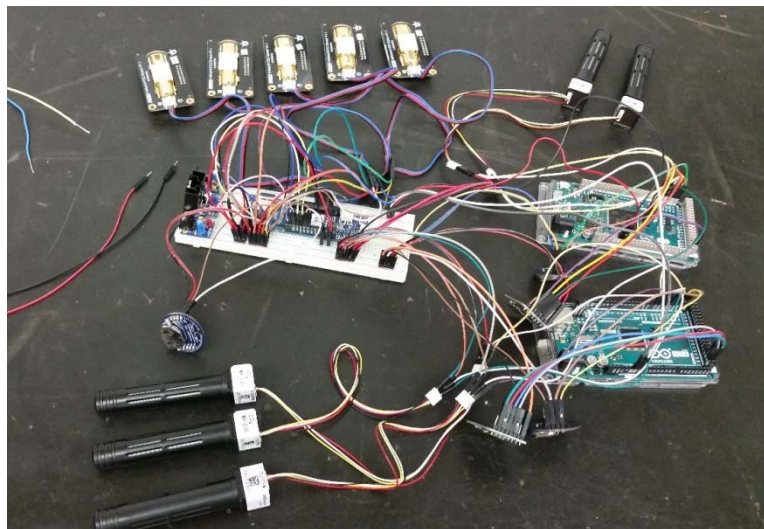


Figure 5. Sensors connected to Arduino microcontrollers

3.4 Experimental Methodology

The following CO₂ concentrations were used with a one hour dosing time to ensure chamber concentration stability had been reached: 300 ppm, 1771 ppm, 2530 ppm, and 3880 ppm. The test includes an evaluation of the accuracy, linearity, repeatability, and hysteresis of the CO₂ sensors.

The accuracy and linearity were evaluated using increasing and decreasing step changes of CO₂ concentration dosing. Repeatability was evaluated using multiple measurements of the same concentration and direction of step change. Hysteresis was evaluated by comparing the measurements of increasing and decreasing step changes at the same concentration.

Figure 6 shows ten CO₂ sensors of both types A and B connected to Arduino microcontrollers, along with real-time clocks and SD card readers for data logging placed in the chamber for testing.

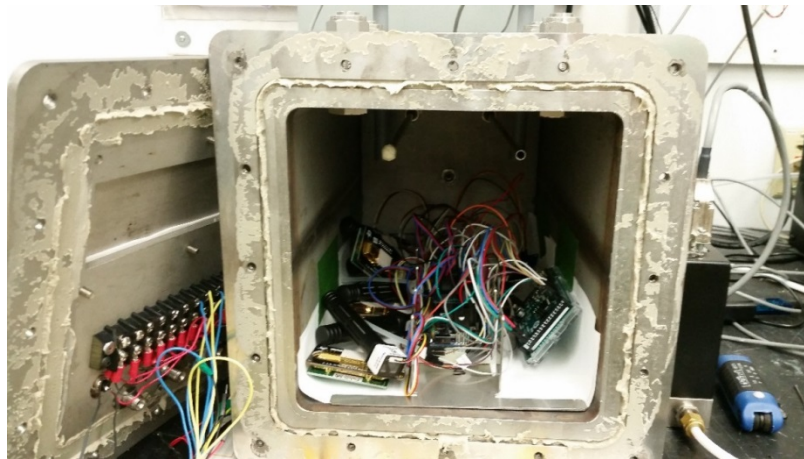


Figure 6. Sensors and data acquisition hardware placed in the test chamber

A gas mixture of CO₂ and nitrogen was injected into the sealed test chamber using calibrated gas cylinders, as illustrated in Figure 7. The figure shows the dosing of a 300 ppm CO₂ gas mixture from a calibrated gas cylinder at a flow rate of 2.5 L/min with 45 psi regulated gas pressure, as per the procedure for the operation of the test chamber for CO₂ sensor calibration.

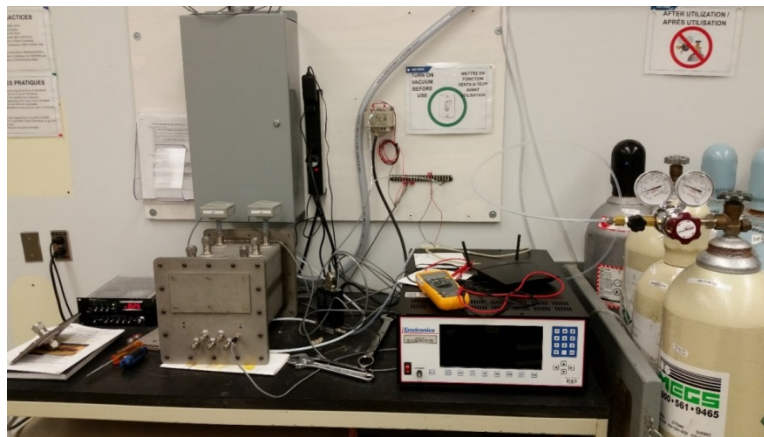


Figure 7. 300 ppm CO₂ cylinder connected to mass flow controller and chamber

4 Results

This section begins with a short presentation of results from testing the chamber performance to verify that it was well-sealed, followed by a comparison between reference CO₂ sensors and calibrated concentration gas values. Following this, sample results from the testing of the low-cost CO₂ sensors are presented, along with detailed analysis of steady-state accuracy, hysteresis, and repeatability. The results are summarized using statistical methods such as standard deviation and binned distributions. The primary data is included in Appendix B.

4.1 Verifying Chamber Performance

To ensure the test chamber was well-sealed and not admitting air from the laboratory room, a 1771 ppm CO₂ concentration was injected for a period of one hour at a flow rate of 2.5 L/min and then later increased to 5 L/min, 7.5 L/min, and 10 L/min on one hour intervals. Results showed no notable change in sensor readings for the whole test duration, indicating that the chamber is well-sealed and there is no measurable unintended inward leakage. Figure 8 shows CO₂ concentration readings of three sensors during the leakage test. The consistency in the measured CO₂ concentration demonstrates the reliability of the calibration chamber. The results obtained from this procedure support the application of the assumption that the CO₂ concentration in the test chamber during dosing approaches a steady-state value equal to the concentration of the calibrated cylinder.

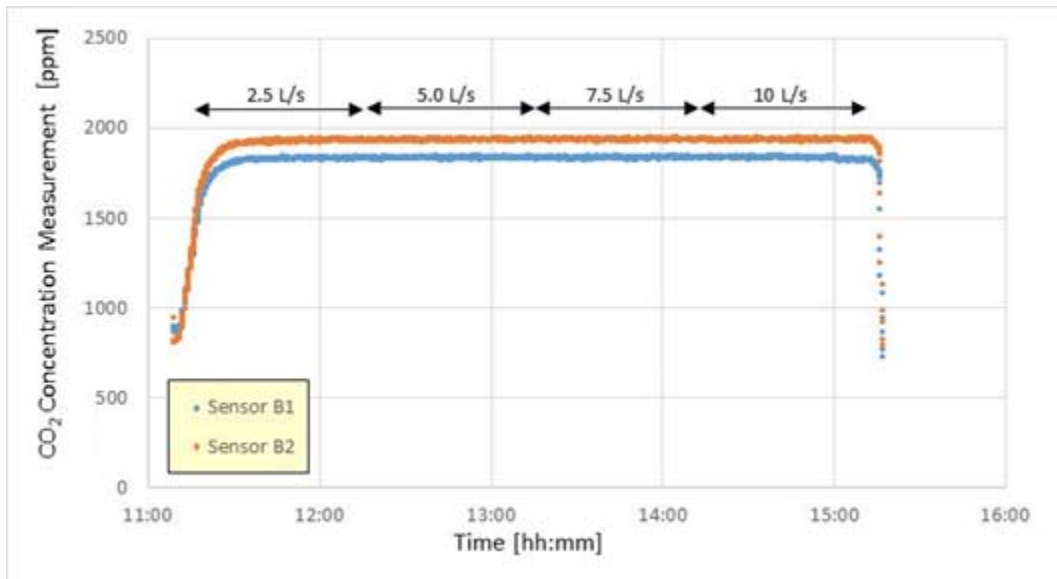


Figure 8. Increasing calibrated gas flow rate test

4.2 Reference CO₂ Sensor Calibration

The Vaisala reference CO₂ sensors were subjected to 300 ppm, 1050 ppm and 2550 ppm to establish calibration curves of their responses. Figure 9 shows the relationship between the injected CO₂ concentration and the output voltage of each Vaisala GMD20 sensor. The tabular data for this calibration can be found in Table 1 in Appendix A.

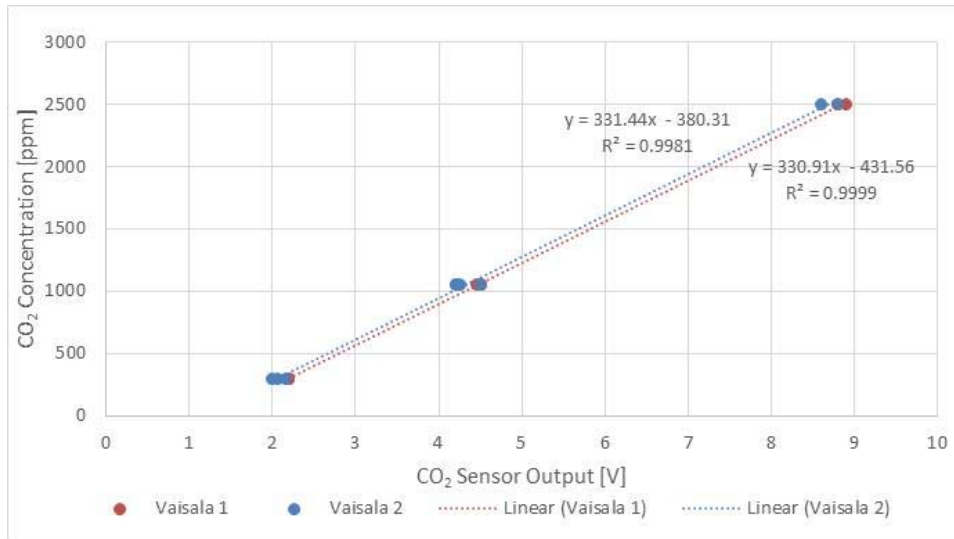


Figure 9. Vaisala GMD20 sensor readings

Both readings had an R^2 value close to unity for a linear fit, which demonstrates that the linearity of both sensors is very good. Therefore, the actual CO₂ concentration could be confirmed by measuring the output voltage of these sensors and obtaining the corresponding CO₂ concentration from Figure 9.

4.3 CO₂ Sensor Testing Sample Results

A sample result from preliminary testing of sensor type C is shown below in Figure 10. From this figure, it is evident that the sensor could not provide a useful steady state response. Several other preliminary attempts were conducted to try to get a useful response from this sensor, but they did not succeed.

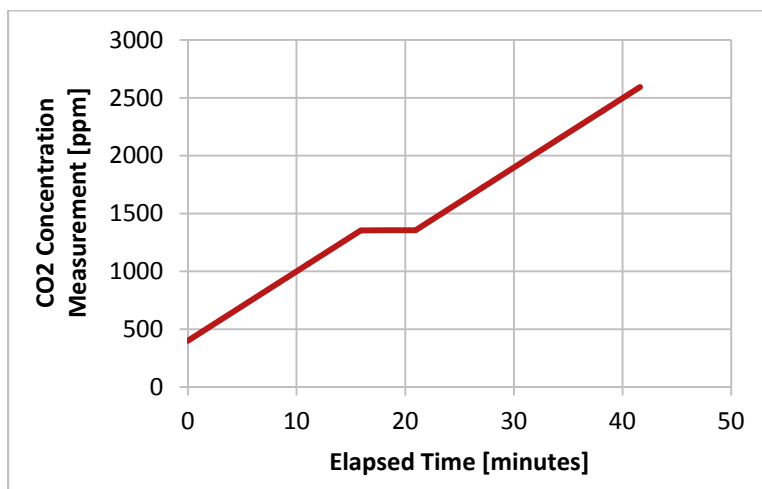


Figure 10. Sensor type C sample response to increasing CO₂ dosing up to 1050 ppm

For the detailed analysis, three days of testing were conducted. Each day, four concentrations were dosed: 300 ppm, 1550 ppm, 2500 ppm, and 3880 ppm. The first dosage concentration was 300 ppm. The concentration was raised every hour, until the maximum concentration of 3880 ppm was dosed. After an hour of dosing 3880 ppm, the concentration was decreased every hour, until the minimum concentration of 300 ppm was dosed. After an hour of dosing 300 ppm for a second time, the experiment was completed for the day. This process was repeated all three days.

The experimental results from day 1 are illustrated in Figure 11 and Figure 12 for type A sensors and type B sensors, respectively. Figure 11 and Figure 12 show the CO₂ concentration stepping up and down. Both figures demonstrate an increasing spread in absolute concentration readings at higher CO₂ levels. Despite the fact that the minimum reading threshold of sensor type A is 400 ppm, 300 ppm was included in the test as a starting concentration. Note that for sensor type B, some readings in Figure 12 appear at 0 ppm due a given sensor temporarily not returning a value to the microcontroller. These values were filtered out in the calculations and could be filtered out in a device control strategy as well.

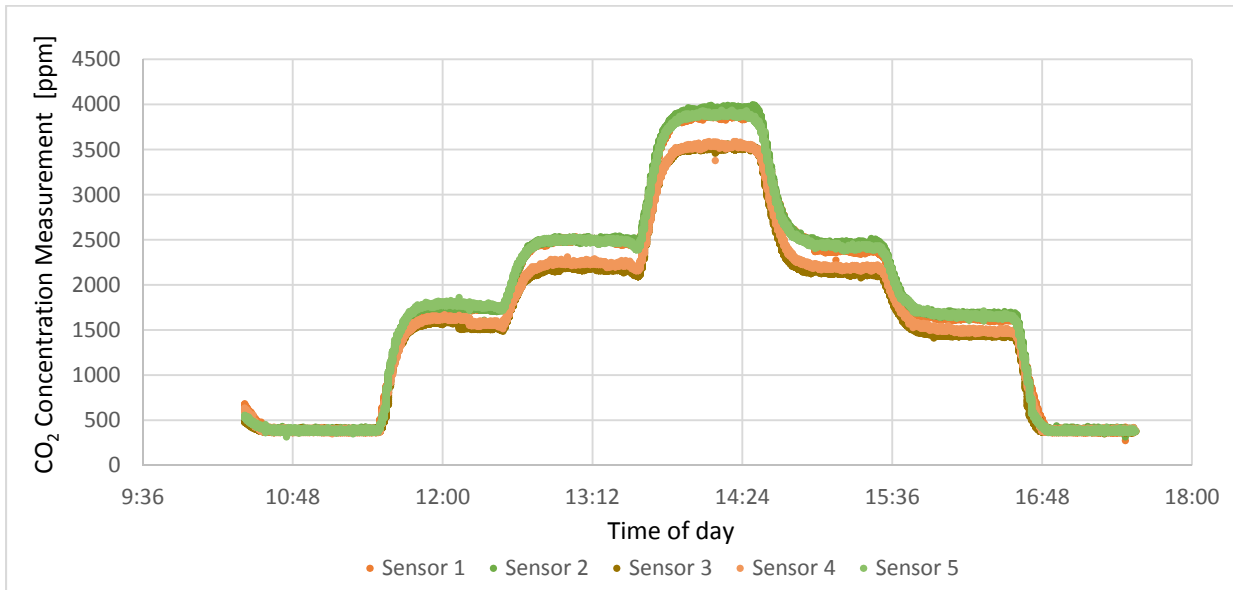


Figure 11. Sensors type A readings, day 1

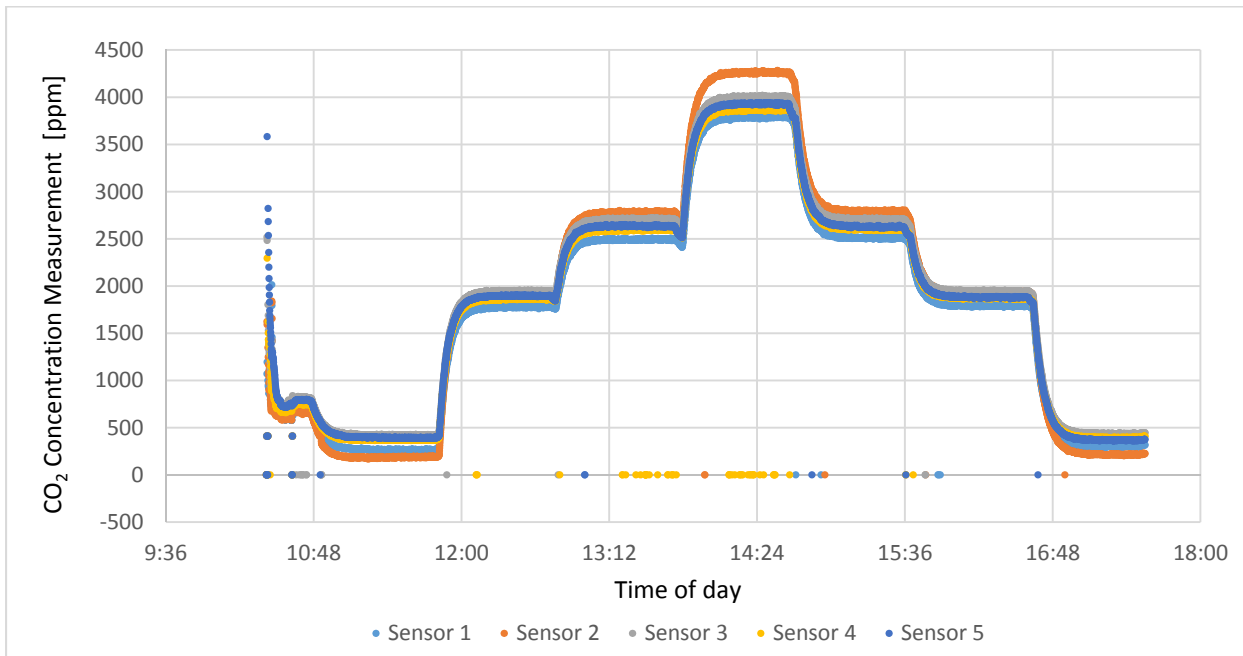


Figure 12. Sensor type B readings, day 1

4.4 Steady-State Accuracy

At each concentration value, an average of 30 minutes of stable readings were taken to calculate the steady state response. These have been calculated according to Equation 1:

$$\bar{X} = \frac{\sum X}{N}$$

Equation 1

Where:

\bar{X} : Average Measurement

X : Measurements

N : Number of samples

Figure 13 and Figure 14 display the average concentration measurement during the 30 minute steady state period for all five sensors of sensor type A and B, respectively.

Figure 15 includes both sensor types and shows the average concentration measurements during the 30 minute steady state period for the three days.

Figure 13 and Figure 14 show a diversion in the measurements from sensor type A and B at high CO₂ concentrations. Figure 13 shows that typically the error margin for sensor type A is greater than 10%, which does not meet the accuracy specified by the manufacturer: ± (50ppm + 3% reading). Figure 14 shows that sensor type B is more accurate and generally meets the accuracy specified by the manufacturer which states that the accuracy is 200 ppm (10% of the concentration range, 400-2000 ppm).

Figure 13 shows that the five type A sensors generally measured values below the perfect agreement line. Approximately 66% of the average sensor measurements were lower than the concentration that was supplied to the chamber via the calibrated CO₂ cylinders and about 50% of the average sensors' measurements were between the 10% error margins. On the other hand, Figure 14 shows that the five type B sensors generally measured values above the perfect agreement line. Approximately 86% of the average sensor measurements were above the concentration that was supplied to the chamber via the calibrated CO₂ cylinders and about 62% of the average sensors' measurements were between the 10% error margins, indicating that sensor type B is more accurate.

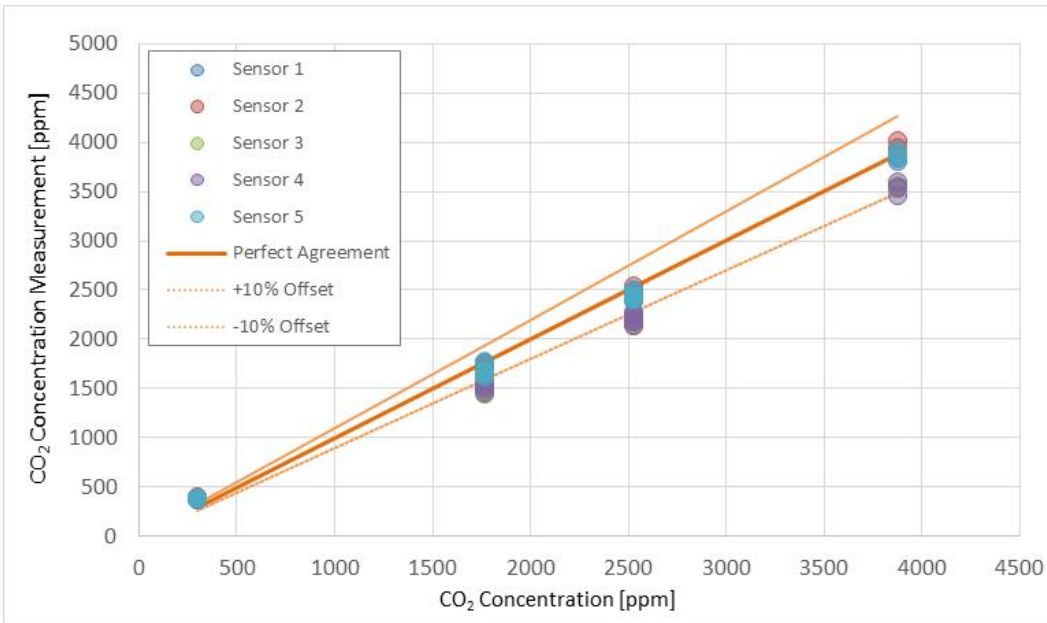


Figure 13. Sensor type A readings, all three days

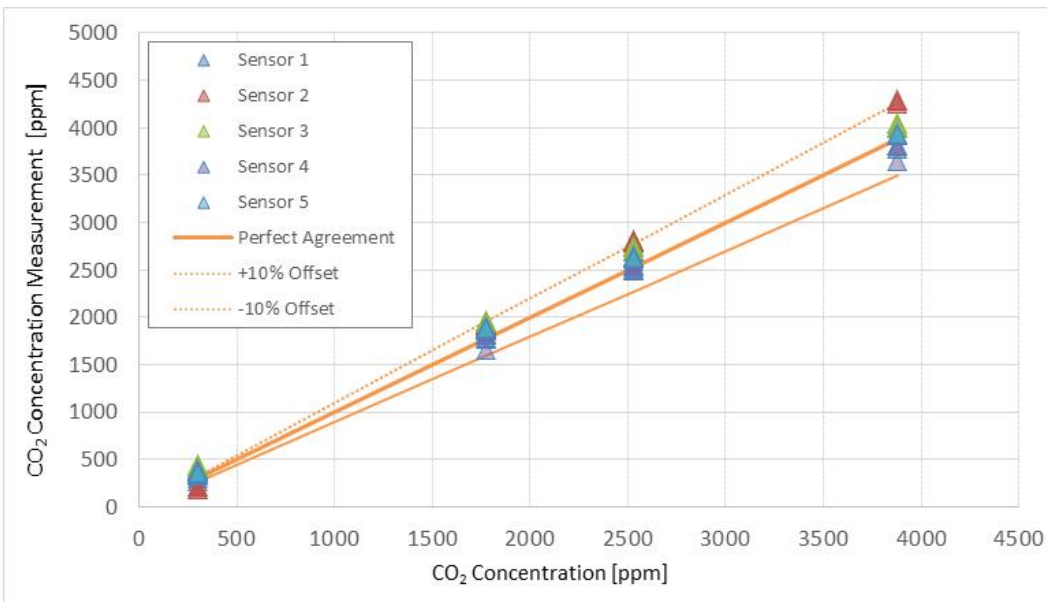


Figure 14. Sensor type B readings, all three days

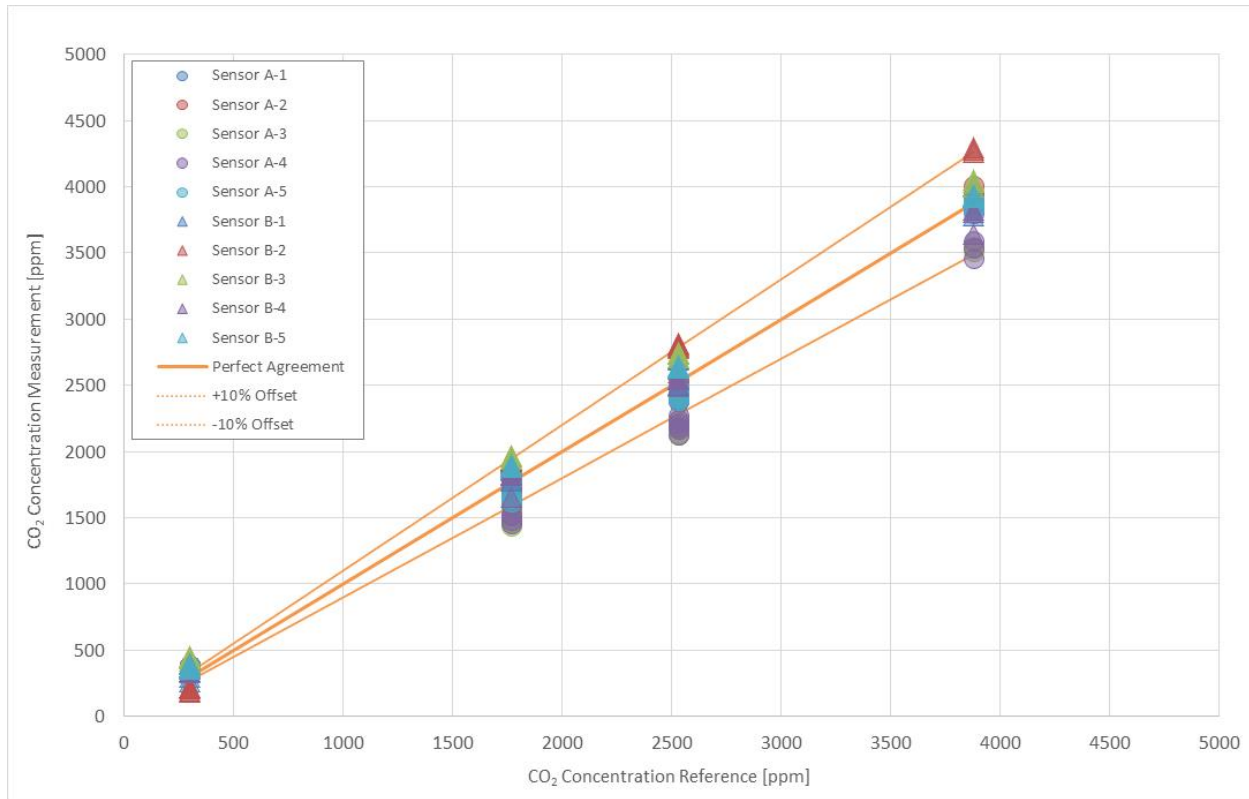


Figure 15. Sensors types A & B readings, all three days

4.4.1 Detailed Accuracy Analysis

Sensor accuracy is calculated as the deviation of the measured sensor value from the calibrated gas CO₂ concentration. Equation 2 and Equation 3 are utilized to calculate the error as a percentage and the deviation error, respectively.

$$Error (\%) = \left(\frac{\text{measured } CO_2 \text{ concentration}}{\text{actual } CO_2 \text{ concentration}} - 1 \right) \times 100\% \quad \text{Equation 2}$$

$$Error (ppm) = \text{measured } CO_2 \text{ concentration} - \text{actual } CO_2 \text{ concentration} \quad \text{Equation 3}$$

Figure 16 and Figure 17 illustrate the percentage error of sensor type A and B for all CO₂ concentrations used during the three days of testing.

Figure 16 shows that sensor type A had high percentage errors at 300 ppm since its minimum operating threshold is 400 ppm. Also, Figure 16 shows that sensors 3 and 4 had the highest percentage errors amongst the group, at more than 10%. Sensors 1, 2, and 5 demonstrated more accuracy in their readings, with less than 10% error.

Figure 17 illustrates that the percentage errors of sensor type B at the low concentrations of 300 ppm are high due to a bottoming-out of the sensor readings below 300 ppm. This is to be expected, as the sensors are said to only be accurate to specifications down to 400 ppm. The overall percentage error is within 10% for 1771 ppm, 2530 ppm, and 3880 ppm CO₂ concentrations. Sensors 1, 4, and 5 demonstrated more accuracy in their overall readings compared to sensors 2 and 3.

Figure 18 and Figure 19 show the deviation error of sensor type A and B for all CO₂ concentrations used during the three days of testing.

Figure 18 illustrates that sensor type A had high deviation errors and typically under-reported the actual CO₂ concentrations. The deviation errors were small for sensors 1, 2, and 5; the maximum recorded measurement was below 150 ppm. By contrast, the deviation errors for sensors 3 and 4 were typically between -300 ppm and -400 ppm at the high CO₂ concentrations of 2530 ppm and 3880 ppm.

Figure 19 shows that sensor type B had high deviation errors for the high CO₂ concentration of 3880 ppm. In general, all type B sensors over-report the actual CO₂ concentrations. The deviation errors were smaller for sensors 1, 3, 4, and 5. Whereas, the error was up to 400 ppm for sensor 2 at the high CO₂ concentration of 3880 ppm.

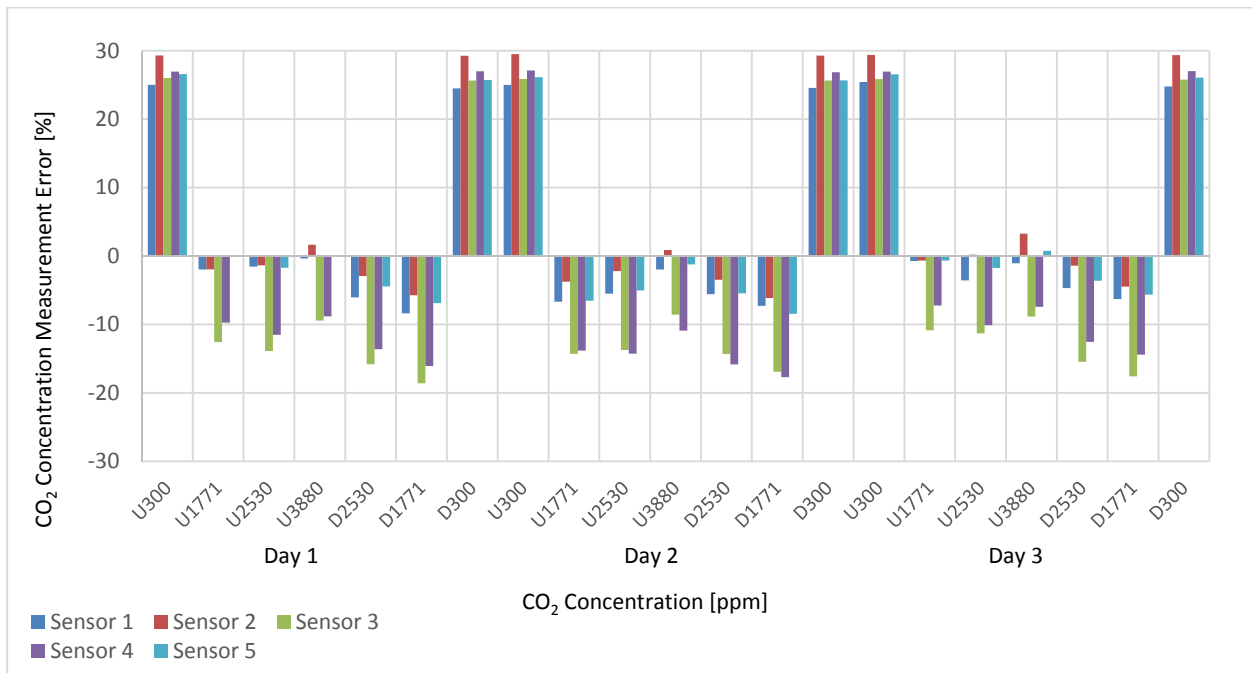


Figure 16. Sensor type A percentage error

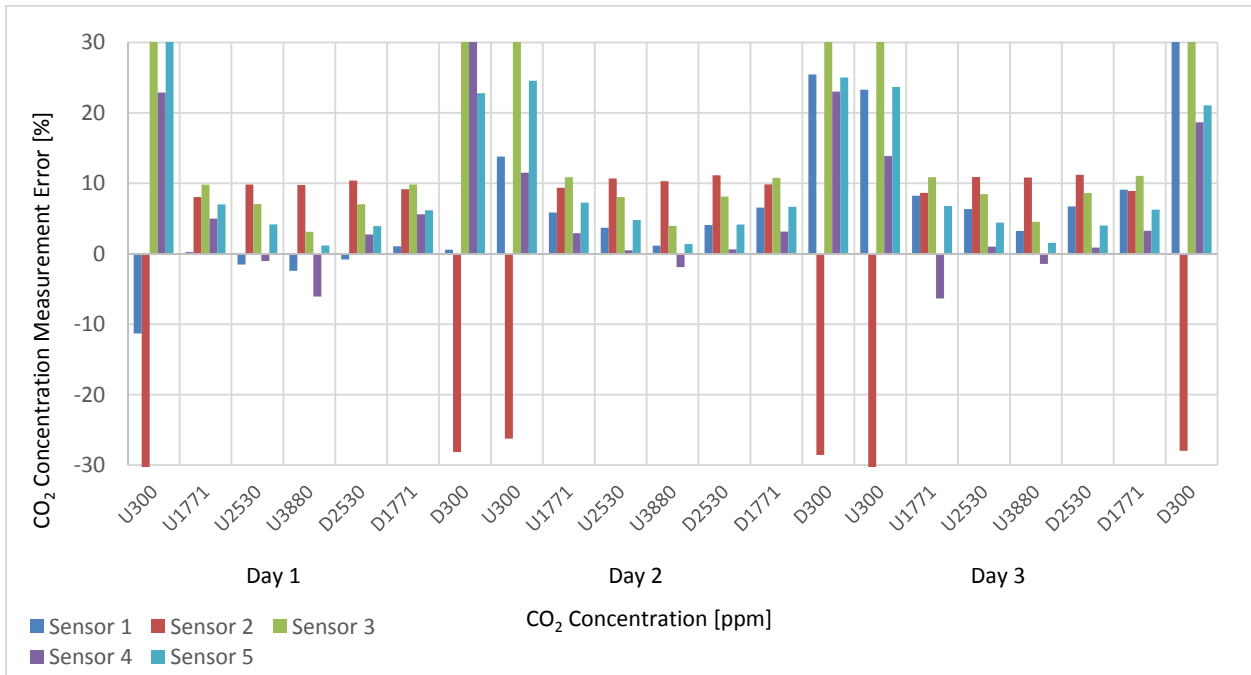


Figure 17. Sensor type B percentage error

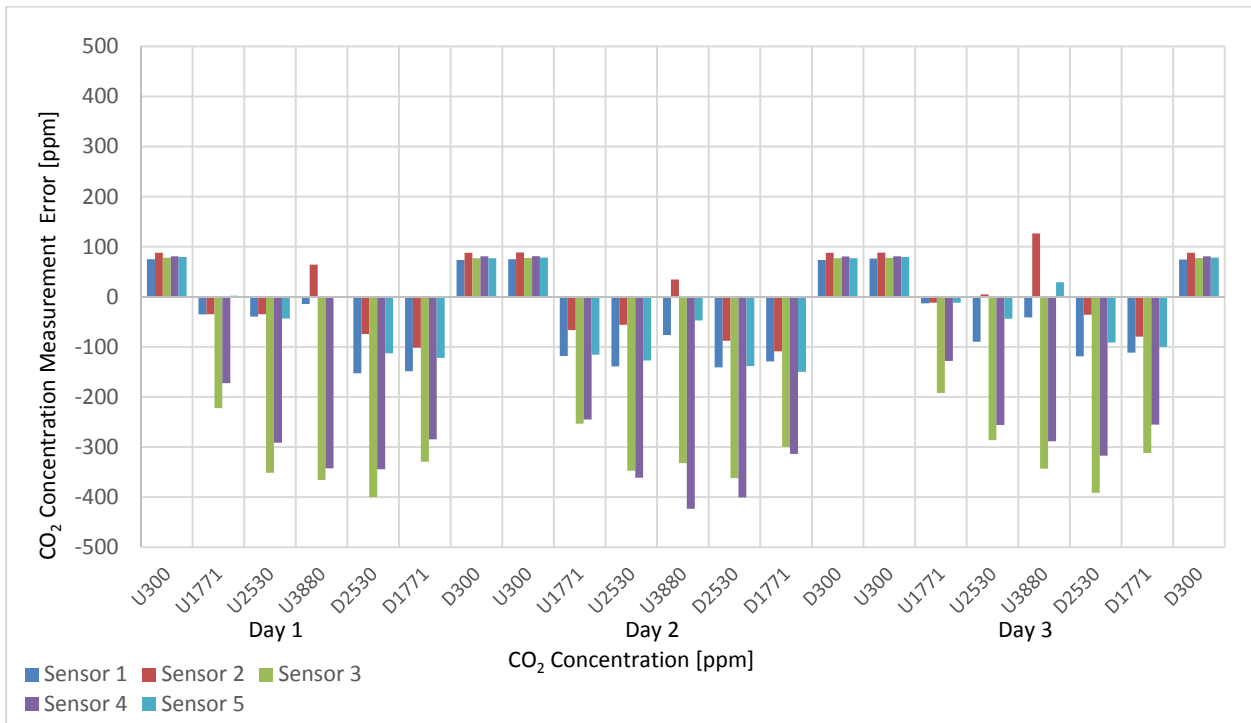


Figure 18. Sensor type A deviation error

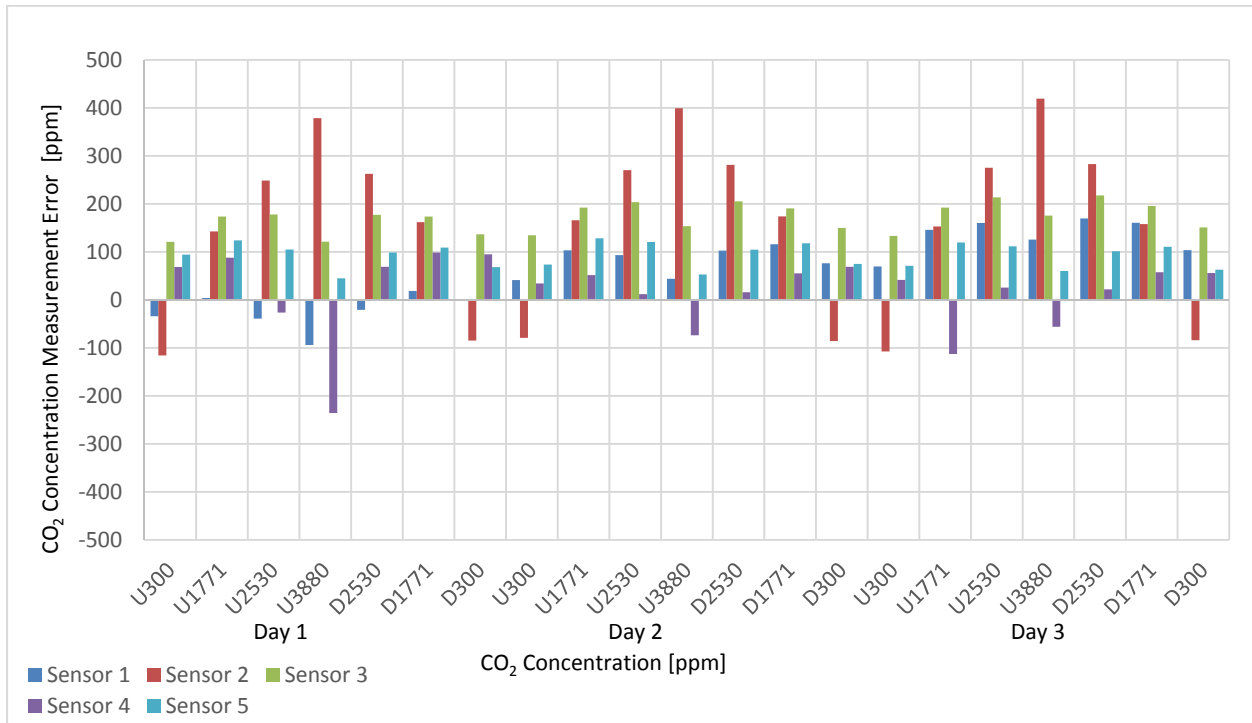


Figure 19. Sensor type B deviation error

For further analysis of accuracy and deviation errors for both sensors, histograms were produced. Figure 20 and Figure 21 display the distribution of percentage error and deviation error of sensor type A, respectively. Figure 22 and Figure 23 display the distribution of percentage error and deviation error of sensor type B, respectively. The histogram bins include the values which fall between the value of their label and the value of the label directly lower. For example, a bin with a label of -10% includes sample values greater than -20% and less than or equal to -10%. Similarly, a bin with a label of -200 ppm includes sample values greater than -300 ppm and less than or equal to -200 ppm.

The percentage error charts show that sensor type A has 52 samples between -10 and +10% and sensor type B has 65. For both sensors, the error outside of the range of -20 to +20% is all attributed to readings at the concentration of 300 ppm, where neither sensor is expected to be accurate, since the value is lower than 400 ppm. The deviation error charts highlight how the readings from sensor type A are strongly biased towards underreporting and overall have more frequency of readings further off by +/-300 ppm compared to sensor type B. The deviation errors also show that sensor type A has less errors in the -200 to 200 ppm range with 78 samples compared to 91 for sensor type B.

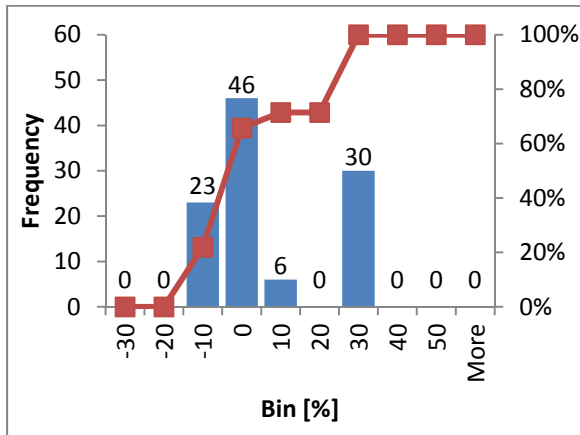


Figure 20. Sensor type A percentage error analysis

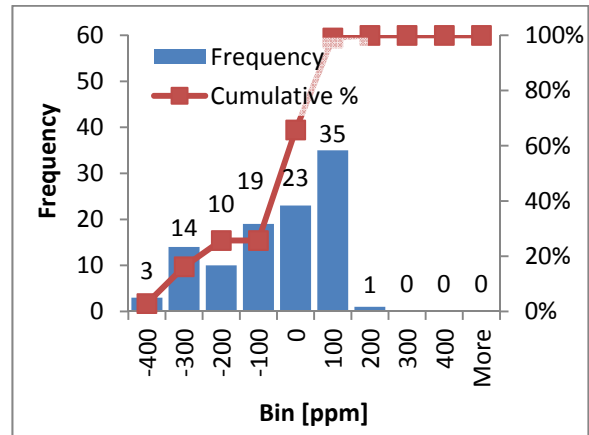


Figure 21. Sensor type A deviation error analysis

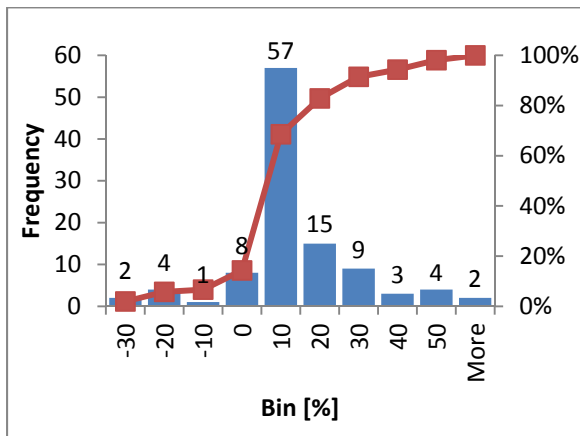


Figure 22. Sensor type B percentage error analysis

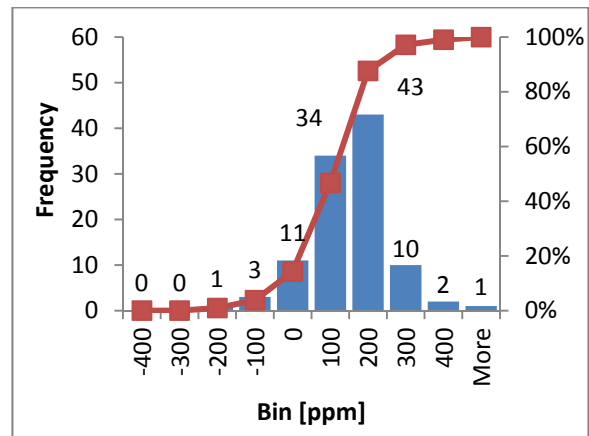


Figure 23. Sensor type B deviation error analysis

4.5 Hysteresis

Low hysteresis is the ability to produce a very close output when exposed to the same conditions from increasing and decreasing directions [5]. Equation 4 was utilized to calculate the difference between the forward measurement and the reverse measurement at CO₂ concentrations 300 ppm, 1771 ppm, and 2530 ppm.

$$\text{Hysteresis error (ppm)} = \text{stepping up measured CO}_2 \text{ concentration} - \text{stepping down measured CO}_2 \text{ concentration}$$

Equation 4

Figure 24 and Figure 25 display histograms that have been used to summarize the hysteresis results. More detailed results are included in Appendix B.

It must be noted that the histograms are based only on 1771 ppm and 2530 ppm for Sensor A, as it does not report CO₂ concentrations accurately under 400 ppm. Figure 24 shows that the hysteresis errors for sensor type A are within 50 ppm, 100 ppm, and 150 ppm.

In a similar way, Figure 25 shows that the hysteresis errors for sensor type B are within -150 ppm, -50 ppm, 0 ppm, and 50 ppm.

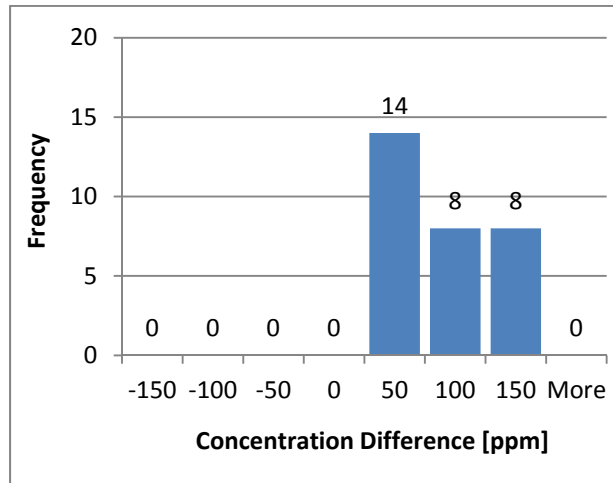


Figure 24. Sensor type A hysteresis analysis

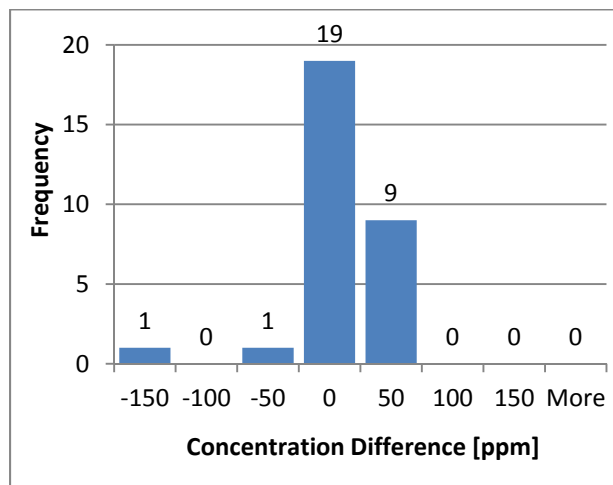


Figure 25. Sensor type B hysteresis analysis

Figure 25 shows that the hysteresis for sensor type B is within 0-50 ppm for 63.3% of the test points, whereas the hysteresis for sensor type A is commonly more than 50 ppm (53.3% of the time), with the maximum hysteresis being 127 ppm. For sensor type A, eight test points had a hysteresis of between 100 ppm and 150 ppm, showing that this sensor type exhibits a notably higher magnitude of hysteresis than sensor type B.

4.6 Repeatability

Repeatability is the capacity of a sensor to give the same output when exposed to the same conditions from the same direction [5]. Repeatability has been calculated as the difference between two increasing or two decreasing measurements of different instances for the same CO₂ concentrations for 300 ppm, 1771 ppm, and 2530 ppm. Equation 5 represents the equation utilized to calculate the repeatability error.

$$\text{Repeatability error (ppm)} = \text{stepping up(down) measured value day 1} - \text{stepping up(down) measured value day 2}$$

Equation 5

Figure 26 shows sensor type A data for all of the concentrations in both directions, up and down. In the legend, 'U' corresponds to up or increasing concentration and 'D' corresponds to down or decreasing concentration. The data is sorted so that bars that represent comparable conditions for repeatability are adjacent to one another, and each sensor is represented individually with all concentrations in both directions. The graph can be read by looking at the 3 trials or "days" for a given sensor and concentration and observing the variation or agreement between the 3 corresponding bars. For example, Figure 26 shows that the repeatability at 1771 ppm was much closer for the downward direction than the upward direction. Overall, all repetitions of sensor type A appear to have similar repeatability.

Similar to the sensor type A repeatability analysis, Figure 27 shows sensor type B repeatability data for all of the concentrations in both increasing and decreasing directions. In contrast to sensor type A, sensor type B did exhibit some variation in the degree of repeatability amongst the sensor repetitions. For example, sensors 2, 3, and 5 demonstrated consistent readings for 1771 ppm CO₂ concentrations, whereas sensors 1 and 4 had wider variations in readings for 1771 ppm. Moreover, sensor 1 had the least consistent behavior amongst the group at all CO₂ concentrations.

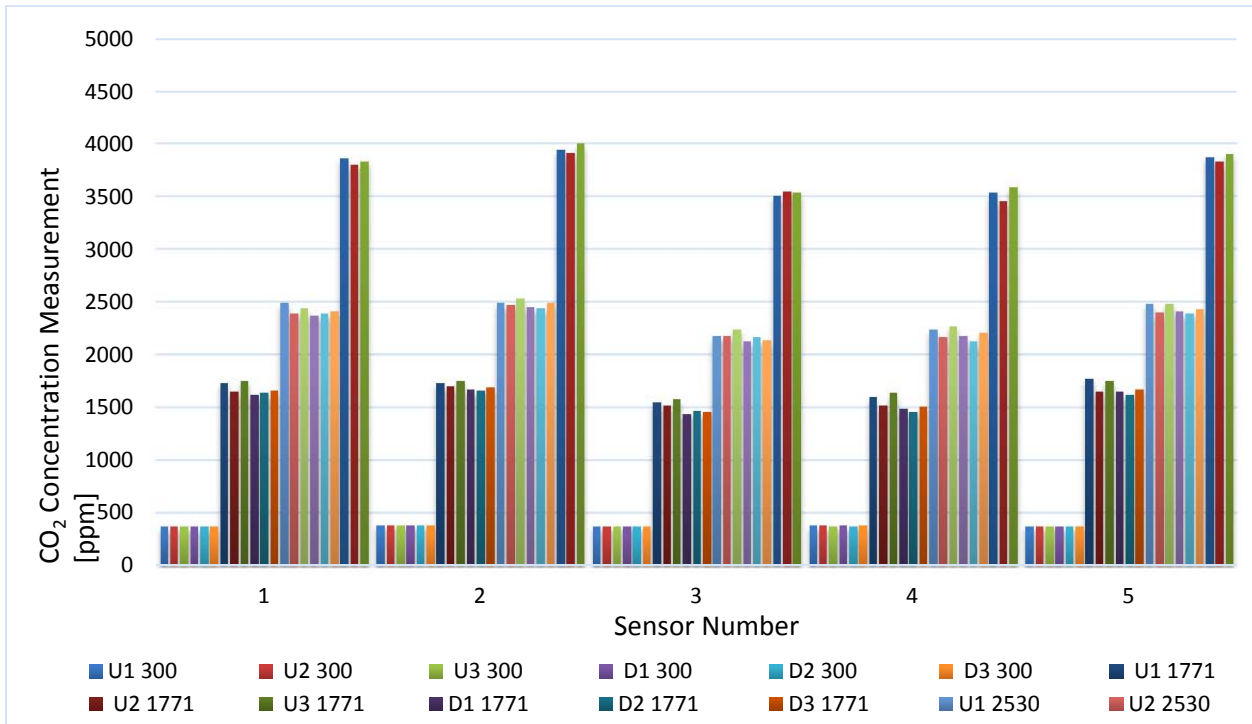


Figure 26. Sensor type A repeatability

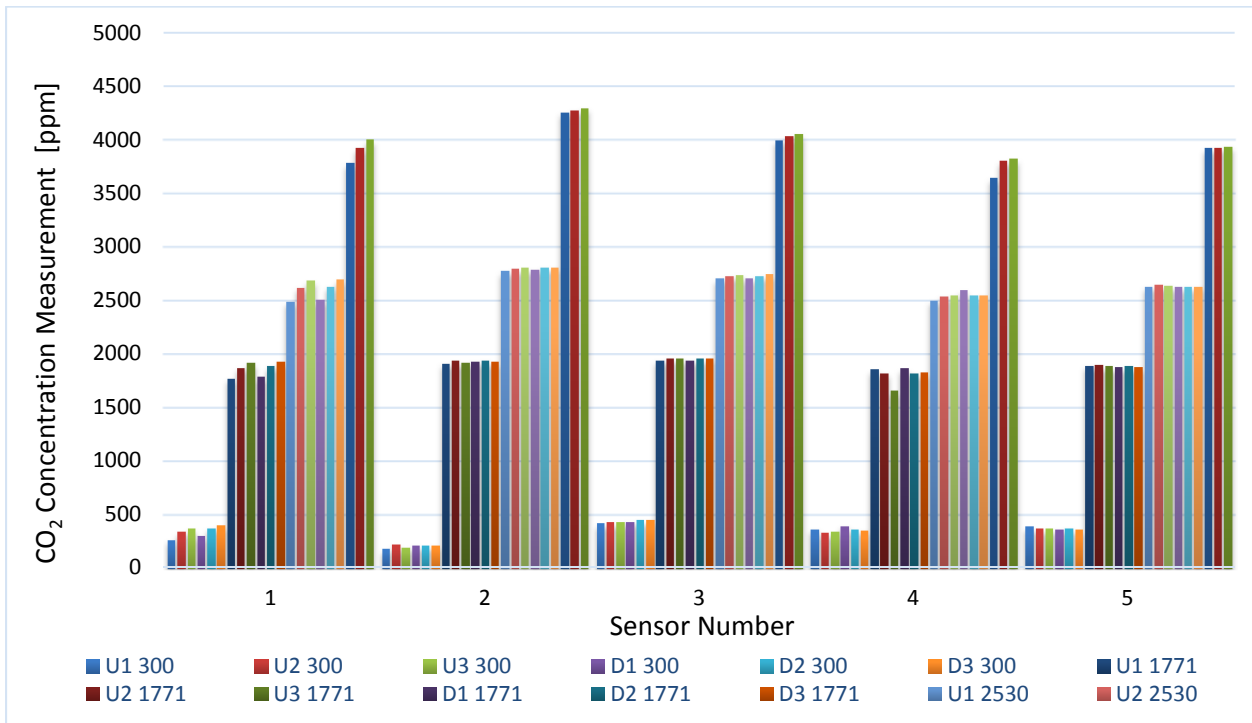


Figure 27. Sensor type B repeatability

The data from Figure 26 and Figure 27 are summarized with histograms in Figure 28, Figure 29, Figure 30, and Figure 31 to enable a more detailed interpretation of the results. The histograms show that for type A sensors nearly all of the repeatability errors are less than 100 ppm, with the majority being below 50 ppm. The histograms also show that for sensor type B nearly all of the repeatability errors are less than 50 ppm.

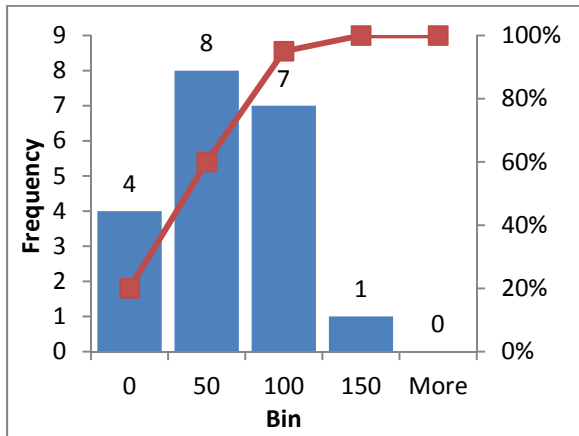


Figure 28. Sensor type A repeatability analysis (increasing)

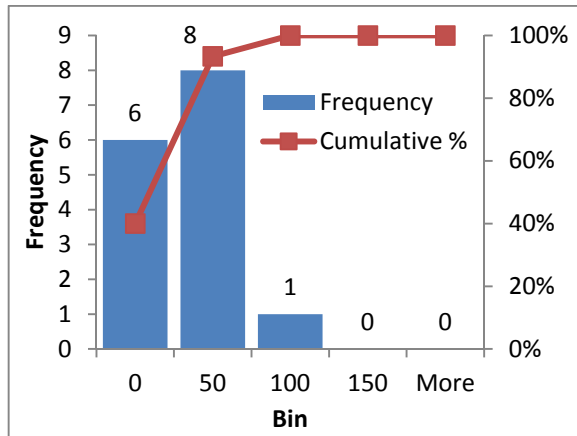


Figure 29. Sensor type A repeatability analysis (decreasing)

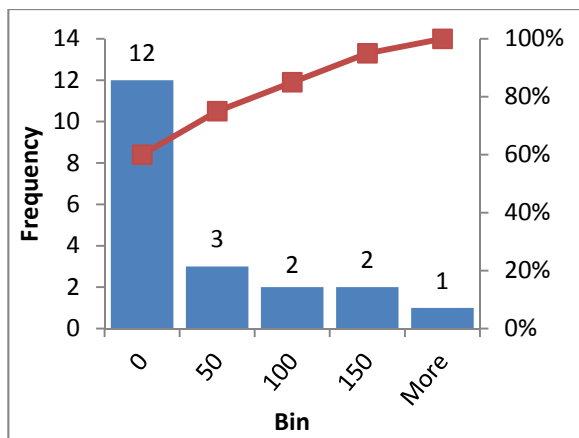


Figure 30. Sensor type B repeatability analysis (increasing)

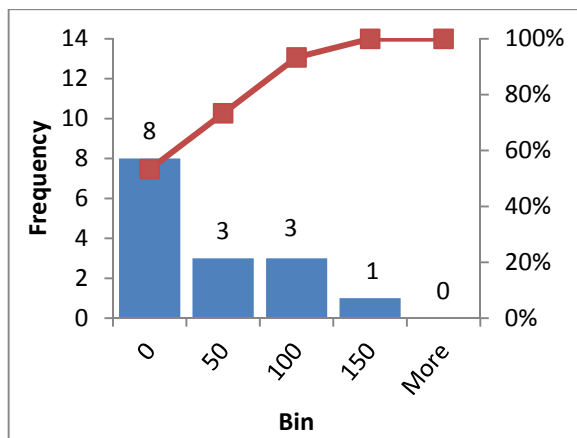


Figure 31. Sensor type B repeatability analysis (decreasing)

4.6.1 Standard Deviation Analysis

Figure 32 and Figure 33 illustrate the standard deviation of sensor types A and B, respectively.

Figure 32 shows that some type A sensors have a standard deviation of approximately 50 ppm but as low as 10 ppm for some readings. For many of the sensors, repeatability in the upward direction had more error. Repeatability was occasionally worse for the 3880 ppm since the results are presented in absolute terms.

Figure 33 shows that type B sensors 2, 3, and 5 had low repeatability errors and hence consistent behavior, whereas, sensor 1 had the highest deviation errors amongst the group. Sensor 4 had poor repeatability for a couple concentrations while the rest had high repeatability.

Figure 32 and Figure 33 demonstrate that the sensor type B had better performance in terms of repeatability than sensor type A.

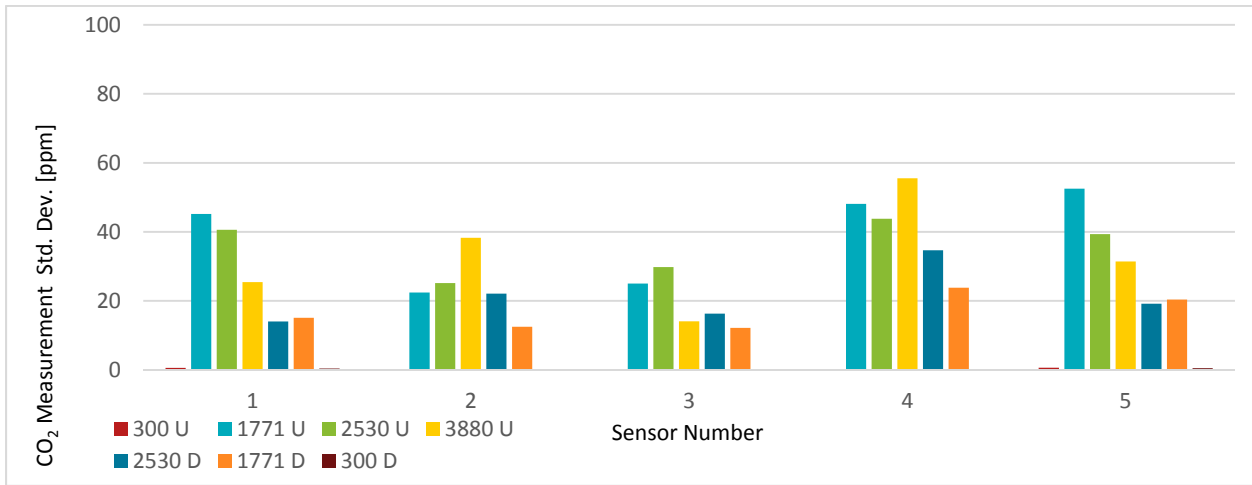


Figure 32. Sensor type A standard deviation

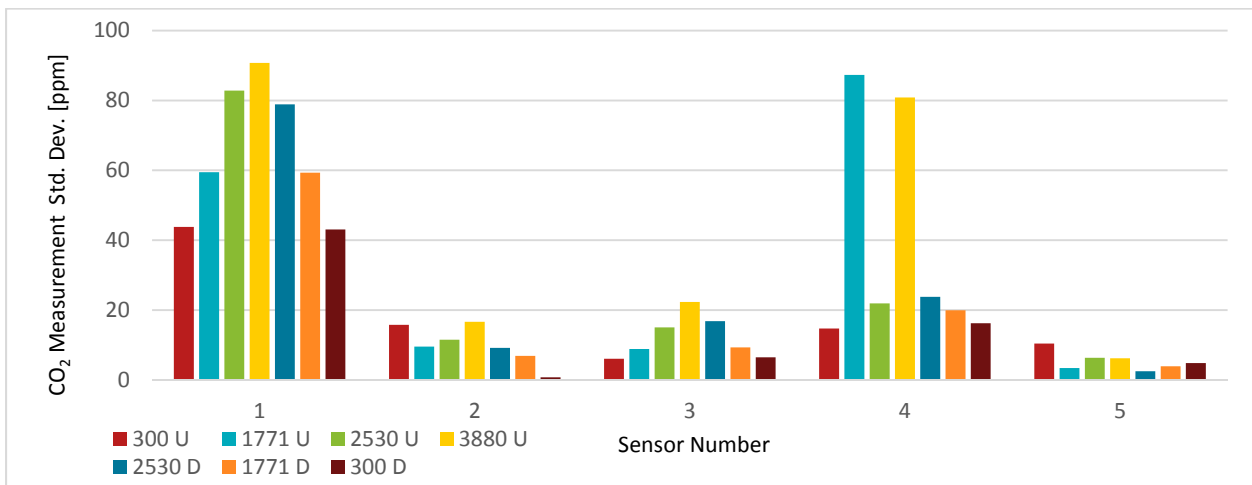


Figure 33. Sensor type B standard deviation

5 Discussion

The apparatus used for the experimental testing of the carbon dioxide sensors was successfully verified as being capable of delivering the calibrated gas concentrations accurately to the test chamber. It was possible to verify the accuracy and consistency of the desired conditions using the Vaisala GMD20 carbon dioxide sensors.

The results of testing the two sensors under consideration show more variation within sensor readings of type A compared to type B. Sensors of type B showed more consistency in their overall behavior. Both sensors' readings had high diversions for the highest concentrations of CO₂, 3880 ppm. This was to be expected since both specifications have quoted uncertainties related to percentage of reading.

The steady-state analysis revealed that sensor type A tends to under-report the CO₂ concentration readings, whereas most type B sensors tend to over-report the concentrations. These results suggest that more accurate relationships between the sensor output and actual CO₂ concentration are possible for each sensor type without individual sensor calibration. This could be achieved through a bulk calibration based on a systematic bias attributed to a given sensor type; however, it may not be necessary for the application of the sensors to demand-controlled ventilation.

The accuracy analysis illustrated that both sensors had high errors at 300 ppm CO₂ concentration since neither is intended to function accurately below 400 ppm. The error at 300 ppm appeared in different ways for each sensor. Sensor type A consistently over-reported the concentration by nearly 100 ppm in all cases, suggesting a bottoming out of the reading near 400 ppm, or the bottom of the useable range, which could be expected. In contrast, sensor type B had some readings that were above actual by approximately 100 ppm or less and some below actual by approximately 100 ppm or less. Interestingly, for concentrations other than 300 ppm, the sensor type B readings were consistently below the actual. The sensor type A readings were consistently above the actual for concentration values other than 300 ppm.

Sensor type A had more than 10% offset errors at all CO₂ concentrations. All type B sensors had high percentage errors at 300 ppm as well, however, all type B sensors had less than 10 % offset errors for 1771 ppm, 2530 ppm, and 3880 ppm CO₂ concentrations.

From the perspective of hysteresis, sensor type A had hysteresis errors up to 150 ppm, while the hysteresis errors for sensor type B were mostly within 50 ppm. This shows that sensor type B performs better in terms of hysteresis, delivering more consistent readings regardless of the direction of concentration change.

The repeatability analysis showed that sensor type A had repeatability errors that were mostly less than 100 ppm in the increasing direction and less than 50 ppm in the decreasing direction. Sensor type B had repeatability errors mostly less than 50 ppm in both directions. Once again, this demonstrates that sensor type B exhibits more ability in measuring CO₂ concentrations accurately and reliably.

For further repeatability and analysis, the standard deviation error at all CO₂ concentrations was taken for both sensors. All type A sensors had high deviation errors. On the other hand, one type B sensor had high deviation errors and another one had high deviation errors at 1771 ppm and 3880 ppm CO₂ concentrations.

6 Conclusion

Sensor type B proved to be reliable and suitable based on the results obtained from the three days of experiments. Moreover, it demonstrated consistent and stable behavior. The five type B sensors gave very close readings for CO₂ concentrations of 1771 ppm and 2530 ppm, but their readings have a wide diversion for higher concentration of CO₂ (3880 ppm).

In terms of hysteresis, sensor type B performed better and had hysteresis within 50 ppm compared to sensor type A which had higher overall hysteresis of up to 150 ppm. The repeatability performance was almost the same for sensor types A and B, with ± 100 ppm repeatability error for both. In terms of accuracy, sensor type B proved to be more accurate than sensor type A. When excluding the 300 ppm concentration dosage, approximately 85% of sensor type B measurements were within a 10% error margin, compared to 69% by sensor type A. In terms of absolute accuracy, 85% of the measurements from type B sensors were within ± 200 ppm and only 64% of sensor type A measurements.

Based on the obtained results for sensor type A and B it can be concluded that sensor type B will provide adequate reliability in a DCV system, as approximately 85% of the measurements were within the 10% error margin. In addition, the analysis of the obtained results for sensor type A revealed that caution must be taken when purchasing some CO₂ sensors. Although the manufacturer specified a high degree of accuracy, utilizing this sensor without testing prior to deployment could prove to be detrimental to the functionality of a DCV system, as calibration testing revealed that only 41% of the measurements fell within the specified error range of $\pm(50\text{ppm} + 3\%$ of the reading). Further testing and analysis can be conducted to evaluate the reliability and accuracy of sensor types A and B. The two sensor types can be placed in an inhabited building and the measurements can be monitored to evaluate their performance in a real life environment.

7 Future Work

Due to this work which demonstrates the feasibility of low-cost carbon dioxide sensors operating a demand-controlled ventilation system, a prototype system will be explored in an experimental real building scenario to demonstrate actual operation of a ventilation system. The performance with varying levels of occupancy will be investigated.

Although it was demonstrated that both sensors could be accurate and reliable enough to ensure a low-cost residential demand-controlled ventilation system would work. The error of the sensors would be expected to result in non-ideal air quality or energy performance depending on the type and direction of the error exhibited. It is not well understood how sensor error would impact these factors nor if the effect would be significant. A method to investigate and develop better understanding of this and more objective criteria could be explored.

Acknowledgments

Nicholas Navarre for his work in getting the apparatus functional and developing the data logging capabilities.

References

- [1] D. Etheridge and M. Sandberg, *Building Ventilation: Theory and Measurement*. John Wiley & Sons, Inc., 1996.
- [2] S. S. Shrestha and G. M. Maxwell, “An experimental evaluation of HVAC-grade carbon dioxide sensors - Part 1: Test and evaluation procedure,” *ASHRAE Trans.*, vol. 115, pp. 471–483, 2009.
- [3] P. Fahlen, H. Andersson, and S. Ruud, “Demand Controlled Ventilating Systems Sensor Tests,” 1992.
- [4] W. J. Fisk, D. Faulkner, and D. P. Sullivan, “A pilot study of the accuracy of CO₂ sensors in commercial buildings,” *Proc. IAQ 2007 "Healthy Sustain. Build.*, 2008.
- [5] S. K. Pandey, K. H. Kim, and S. H. Lee, “Use of a dynamic enclosure approach to test the accuracy of the NDIR sensor: Evaluation based on the CO₂ equilibration pattern,” *Sensors*, vol. 7, no. 12, pp. 3459–3471, 2007.
- [6] S. S. Shrestha and G. M. Maxwell, “An experimental evaluation of HVAC-grade carbon-dioxide sensors - Part 2: Performance test results,” *ASHRAE Trans.*, vol. 116, no. 2006, pp. 260–270, 2010.
- [7] S. Shrestha and G. M. Maxwell, “An Experimental Evaluation of HVAC-Grade Carbon-Dioxide Sensors - Part 3: Humidity, Temperature, and Pressure Sensitivity Test Results,” *ASHRAE Trans.*, vol. 116, no. 2, pp. 271–284, 2010.
- [8] “GMD20 Series Carbon Dioxide Transmitters,” Vaisala, 2018.
- [9] DFRobot, “Gravity Analog Infrared CO₂ Sensor For Arduino,” 2018.
- [10] “MH-Z16 Intelligent Infrared Gas Module Manual,” Zhengzhou Winsen Electronics Technology CO., LTD.
- [11] Seeed Studio, “Grove CO₂ Sensor,” 2015.

Appendix A - Reference Sensor Calibration Data

Table 1. Vaisala GMD20 sensor readings

	CO₂ ppm	Output1 (0 - 10V)	Output2 (0 – 10V)
11:05	Atmosphere	2.7	2.67
12:00	300	2.2	2.17
13:00	300	2.2	2.07
13:30	1050	4.5	4.2
14:00	1050	4.5	4.5
14:45	2500	8.8	8.6
15:15	2500	8.9	8.8
15:50	1050	4.46	4.2
16:20	1050	4.5	4.26
17:00	300	2.2	2

Table 2. Sensor specifications

Sensor	Specified Accuracy
Vaisala GMD20	$\pm (40 \text{ ppm} + 2\% \text{ of the reading})$ [8]
Gravity SEN0129	$\pm (50 \text{ ppm} + 3\% \text{ of the reading})$ [9]
Grove MH-Z16	$\pm (50 \text{ ppm} + 5\% \text{ of the reading})$ [10]

Appendix B - Data Tables

B.1 Accuracy

Table 3. Sensor type A standard deviation

CO ₂ Concentration (ppm)	Sensor 1 Dev (ppm)	Sensor 2 Dev (ppm)	Sensor 3 Dev (ppm)	Sensor 4 Dev (ppm)	Sensor 5 Dev (ppm)
300 U	0.6	0.2	0.2	0.2	0.6
1771 U	45.2	22.4	25.0	48.1	52.5
2530 U	40.6	25.2	29.8	43.8	39.4
3880 U	25.4	38.3	14.1	55.5	31.4
2530 D	14.0	22.1	16.3	34.7	19.2
1771 D	15.1	12.5	12.2	23.8	20.4
300 D	0.4	0.1	0.2	0.2	0.5

Table 4. Sensor type B standard deviation

CO ₂ Concentration (ppm)	Sensor 1 Dev (ppm)	Sensor 2 Dev (ppm)	Sensor 3 Dev (ppm)	Sensor 4 Dev (ppm)	Sensor 5 Dev (ppm)
300 U	43.8	15.8	6.1	14.7	10.4
1771 U	59.5	9.6	8.9	87.3	3.4
2530 U	82.8	11.5	15.1	21.9	6.4
3880 U	90.7	16.7	22.3	80.9	6.2
2530 D	78.9	9.2	16.8	23.8	2.5
1771 D	59.3	6.9	9.3	20.0	3.9
300 D	43.1	0.8	6.5	16.3	4.8

Table 5. Sensor type A percentage error

Day	CO ₂ Concentration (ppm)	Sensor 1 Error (%)	Sensor 2 Error (%)	Sensor 3 Error (%)	Sensor 4 Error (%)	Sensor 5 Error (%)
Day 1	U300	25.01	29.32	26.02	26.96	26.57
	U1771	-1.97	-1.96	-12.56	-9.74	0.13
	U2530	-1.56	-1.37	-13.88	-11.51	-1.71
	U3880	-0.37	1.66	-9.43	-8.82	-0.03
	D2530	-6.03	-2.93	-15.81	-13.60	-4.46
	D1771	-8.39	-5.74	-18.59	-16.07	-6.89
Day 2	D300	24.49	29.27	25.64	27.00	25.74
	U300	25.00	29.50	25.89	27.11	26.12
	U1771	-6.67	-3.76	-14.30	-13.83	-6.52
	U2530	-5.49	-2.20	-13.72	-14.28	-5.02
	U3880	-1.97	0.89	-8.56	-10.91	-1.22
	D2530	-5.57	-3.47	-14.31	-15.83	-5.46
Day 3	D1771	-7.28	-6.14	-16.91	-17.70	-8.46
	D300	24.57	29.29	25.64	26.85	25.68
	U300	25.43	29.38	25.86	26.95	26.55
	U1771	-0.74	-0.67	-10.84	-7.23	-0.67
	U2530	-3.55	0.19	-11.31	-10.12	-1.73
	U3880	-1.06	3.26	-8.84	-7.43	0.75
Day 3	D2530	-4.69	-1.41	-15.47	-12.54	-3.61
	D1771	-6.30	-4.48	-17.60	-14.41	-5.64
	D300	24.79	29.36	25.79	27.01	26.07

Table 6. Sensor type A deviation error

	CO ₂ Concentration (ppm)	Sensor 1 Error (ppm)	Sensor 2 Error (ppm)	Sensor 3 Error (ppm)	Sensor 4 Error (ppm)	Sensor 5 Error (ppm)
Day 1	U300	75.03	87.97	78.07	80.88	79.72
	U1771	-34.91	-34.68	-222.39	-172.44	2.30
	U2530	-39.49	-34.70	-351.20	-291.31	-43.34
	U3880	-14.22	64.44	-365.82	-342.29	-1.28
	D2530	-152.62	-74.25	-400.04	-344.18	-112.72
	D1771	-148.51	-101.63	-329.19	-284.67	-122.05
Day 2	D300	73.46	87.80	76.92	81.00	77.21
	U300	75.01	88.50	77.66	81.34	78.37
	U1771	-118.04	-66.51	-253.31	-244.89	-115.52
	U2530	-138.92	-55.78	-347.15	-361.31	-127.07
	U3880	-76.36	34.63	-332.03	-423.32	-47.15
	D2530	-140.92	-87.80	-361.95	-400.40	-138.19
Day 3	D1771	-128.99	-108.72	-299.54	-313.54	-149.77
	D300	73.70	87.88	76.91	80.55	77.03
	U300	76.30	88.14	77.58	80.86	79.64
	U1771	-13.15	-11.82	-192.06	-128.13	-11.85
	U2530	-89.79	4.91	-286.05	-255.96	-43.80
	U3880	-40.99	126.57	-342.88	-288.24	29.28
	D2530	-118.77	-35.59	-391.30	-317.15	-91.22
	D1771	-111.54	-79.36	-311.72	-255.25	-99.96
	D300	74.36	88.08	77.37	81.04	78.20

Table 7. Sensor type B percentage error

Day	CO ₂ Concentration (ppm)	Sensor 1 Error (%)	Sensor 2 Error (%)	Sensor 3 Error (%)	Sensor 4 Error (%)	Sensor 5 Error (%)
Day 1	U300	-11.33	-38.56	40.42	22.89	31.45
	U1771	0.23	8.06	9.80	4.98	7.00
	U2530	-1.54	9.83	7.04	-1.03	4.15
	U3880	-2.42	9.76	3.13	-6.07	1.16
	D2530	-0.81	10.39	7.02	2.74	3.91
	D1771	1.06	9.16	9.82	5.58	6.17
	D300	0.58	-28.16	45.64	31.69	22.80
Day 2	U300	13.80	-26.26	44.91	11.49	24.55
	U1771	5.84	9.38	10.86	2.92	7.25
	U2530	3.69	10.69	8.05	0.48	4.77
	U3880	1.13	10.29	3.96	-1.90	1.37
	D2530	4.07	11.13	8.12	0.63	4.15
	D1771	6.55	9.84	10.78	3.14	6.67
	D300	25.44	-28.58	50.03	23.02	25.01
Day 3	U300	23.30	-35.77	44.47	13.87	23.68
	U1771	8.24	8.64	10.87	-6.35	6.77
	U2530	6.34	10.88	8.45	1.01	4.41
	U3880	3.24	10.81	4.53	-1.44	1.55
	D2530	6.71	11.20	8.61	0.88	4.02
	D1771	9.09	8.92	11.05	3.25	6.25
	D300	34.54	-27.97	50.38	18.65	21.07

Table 8. Sensor type B deviation error

Day	CO ₂ Concentration (ppm)	Sensor 1 Error (ppm)	Sensor 2 Error (ppm)	Sensor 3 Error (ppm)	Sensor 4 Error (ppm)	Sensor 5 Error (ppm)
Day 1	U300	-33.98	-115.68	121.25	68.66	94.36
	U1771	3.99	142.70	173.63	88.23	123.98
	U2530	-38.87	248.74	178.08	-26.11	105.11
	U3880	-94.06	378.71	121.44	-235.62	45.09
	D2530	-20.61	262.92	177.49	69.22	98.80
	D1771	18.78	162.19	173.90	98.90	109.21
	D300	1.74	-84.49	136.92	95.08	68.40
Day 2	U300	41.41	-78.79	134.74	34.47	73.66
	U1771	103.35	166.04	192.27	51.72	128.33
	U2530	93.36	270.35	203.62	12.08	120.65
	U3880	43.94	399.42	153.70	-73.56	53.03
	D2530	102.85	281.56	205.35	15.92	104.92
	D1771	115.94	174.26	190.92	55.56	118.19
	D300	76.33	-85.73	150.08	69.05	75.03
Day 3	U300	69.90	-107.31	133.40	41.62	71.03
	U1771	145.95	153.03	192.54	-112.49	119.91
	U2530	160.51	275.34	213.90	25.61	111.69
	U3880	125.82	419.50	175.81	-56.02	60.31
	D2530	169.87	283.25	217.77	22.23	101.59
	D1771	160.92	158.02	195.61	57.63	110.67
	D300	103.61	-83.91	151.14	55.95	63.20

B.2 Hysteresis

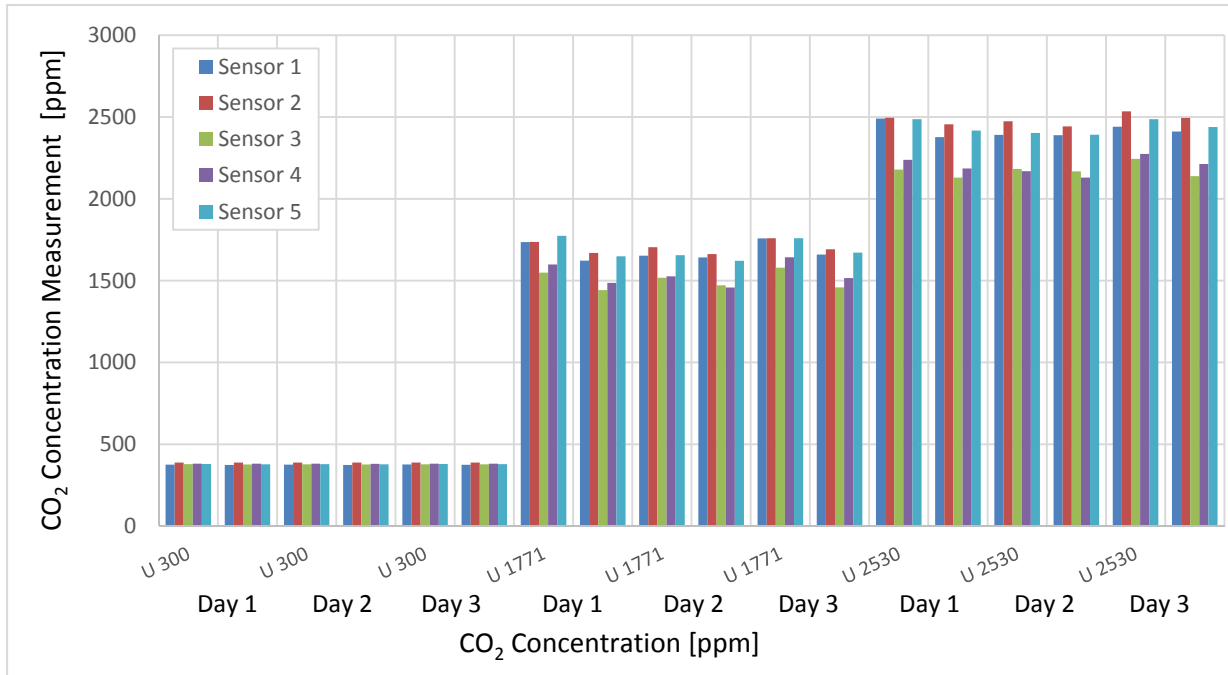


Figure 34. Sensor type A hysteresis

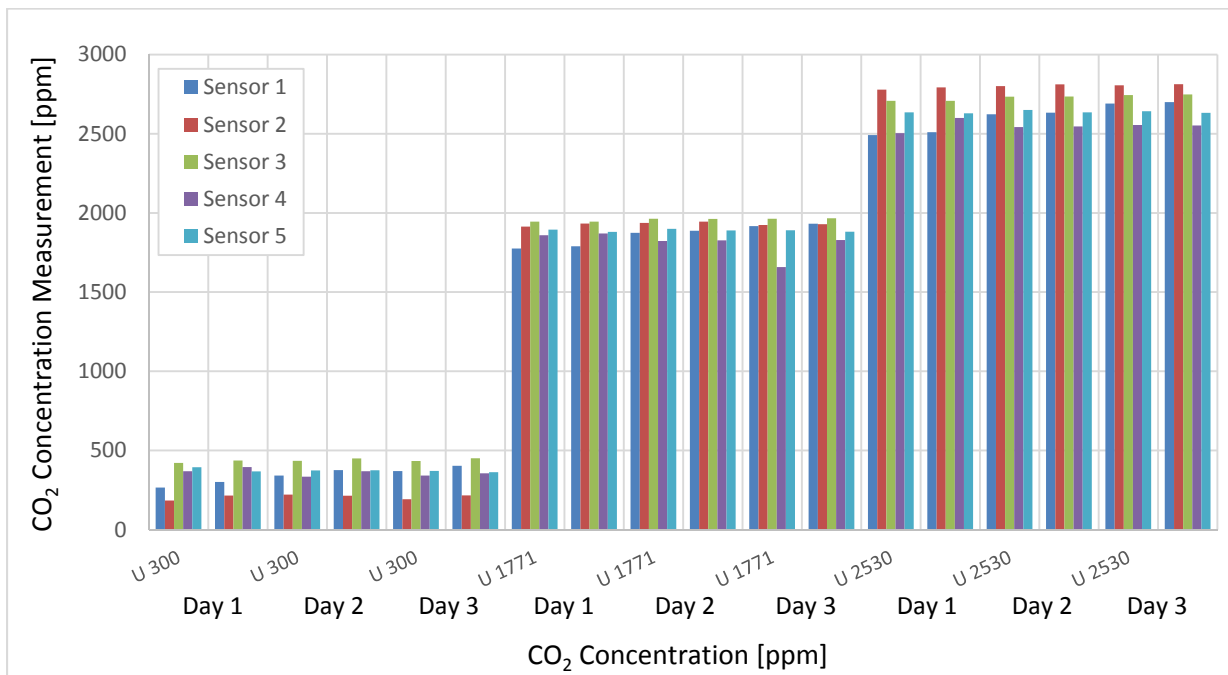


Figure 35. Sensor type B hysteresis

Table 9. Sensor type A hysteresis

	CO ₂ Concentration (ppm)	Sensor 1 Hysteresis (ppm)	Sensor 2 Hysteresis (ppm)	Sensor 3 Hysteresis (ppm)	Sensor 4 Hysteresis (ppm)	Sensor 5 Hysteresis (ppm)
Day 1	300	1.6	0.2	1.1	-0.1	2.5
	1771	113.6	67.0	106.8	112.2	124.4
	2530	113.1	39.5	48.8	52.9	69.4
Day 2	300	1.3	0.6	0.8	0.8	1.3
	1771	11.0	42.2	46.2	68.6	34.2
	2530	2.0	32.0	14.8	39.1	11.1
Day 3	300	1.9	0.1	0.2	-0.2	1.4
	1771	98.4	67.5	119.7	127.1	88.1
	2530	29.0	40.5	105.3	61.2	47.4

B.3 Repeatability

Table 10. Sensor type A repeatability (increasing)

CO ₂ Concentration (ppm)	Sensor 1 Repeatability error (ppm)	Sensor 2 Repeatability error (ppm)	Sensor 3 Repeatability error (ppm)	Sensor 4 Repeatability error (ppm)	Sensor 5 Repeatability error (ppm)
300	0.0	-0.5	0.4	-0.5	1.3
1771	83.1	31.8	30.9	72.5	117.8
2530	99.4	21.1	-4.1	70.0	83.7
3880	62.1	29.8	-33.8	81.0	45.9

Table 11. Sensor type A repeatability (decreasing)

CO ₂ Concentration (ppm)	Sensor 1 Repeatability error (ppm)	Sensor 2 Repeatability error (ppm)	Sensor 3 Repeatability error (ppm)	Sensor 4 Repeatability error (ppm)	Sensor 5 Repeatability error (ppm)
300	-0.2	-0.1	0.0	0.4	0.2
1771	-19.5	7.1	-29.7	28.9	27.7
2530	-11.7	13.6	-38.1	56.2	25.5

Table 12. Sensor type B repeatability (increasing)

CO ₂ Concentration (ppm)	Sensor 1 Repeatability error (ppm)	Sensor 2 Repeatability error (ppm)	Sensor 3 Repeatability error (ppm)	Sensor 4 Repeatability error (ppm)	Sensor 5 Repeatability error (ppm)
300	-75.4	-36.9	-13.5	34.2	20.7
1771	-99.4	-23.3	-18.6	36.5	-4.3
2530	-132.2	-21.6	-25.5	-38.2	-15.5
3880	-138.0	-20.7	-32.3	-162.1	-7.9

Table 13. Sensor type B repeatability (decreasing)

CO ₂ Concentration (ppm)	Sensor 1 Repeatability error (ppm)	Sensor 2 Repeatability error (ppm)	Sensor 3 Repeatability error (ppm)	Sensor 4 Repeatability error (ppm)	Sensor 5 Repeatability error (ppm)
300	-74.6	1.2	-13.2	26.0	-6.6
1771	-97.2	-12.1	-17.0	43.3	-9.0
2530	-123.5	-18.6	-27.9	53.3	-6.1